9th IAA Planetary Defense Conference – PDC 2025
5-9 May 2025, Stellenbosch, Cape Town, South Africa

IAA-PDC-25-01-70

LAMB WAVE DRIVEN TSUNAMI MODEL VALIDATION AND DAMAGE QUANTIFICATION

Mark Boslough [1] **and Vasily Titov**[2]
[1]*Los Alamos National Laboratory, Verification and Analysis, XCP-8, Los Alamos, NM, 87545, 505-999-7756, mbeb@lanl.gov,* [2]*NOAA/Pacific Marine Environmental Laboratory, 7600 Sand Point Way NE, Bldg.3, Seattle, WA, USA 98115-6349,(206)-526-4536, vasily.titov@noaa.gov*

Keywords: *meteotsunami, Laacher See, Meteor Crater, Tunguska, Krakatau*

Abstract

Recent events and research have uncovered an additional potential contributor to global risk estimates from airburst and impact events, the Lamb-wave driven global tsunamis. The 2022 explosion of the Hunga Tonga–Hunga Ha‘apai (HTHH) generated a global Lamb wave that created tsunami waves in the oceans around the world where the water depth provided the conditions needed to create a Proudman resonance, where the velocity of the driving wave (Lamb wave) is close to that of the driven wave (tsunami). We have modeled Lamb-driven tsunamis for HTHH, as well as for the 1883 Krakatau eruption, that match the tsunami observations in terms of timing and amplitude. The simulations provided tsunami model verification and approximate Lamb wave scaling for variable explosion magnitudes. Given the scaling, our simulations have also demonstrated that, counterintuitively, explosions on land can also generate tsunamis. We have run scenarios for the Laacher See volcano, Tunguska airburst, Meteor Crater, and the 2023 PDC scenario with impacts in Dallas and Nigeria. All cases result in global tsunamis of various amplitudes.

For Epoch 1 of 2025 PDC, the risk corridor runs north-south from the Arctic to Antarctic, traversing Europe and Africa. One of the planetary defense data products is a graph of various components of damage (e.g. air blast, heat, etc.) as a function of location along the corridor. Most of the damage is caused by effects that decrease from distance from ground zero, so these graphs tend to strongly reflect the variation in population density along the corridor. By contrast, most of the damage from a global tsunami will be along coastlines that are nowhere near the impact point, even if it is on land. The variation in global damage as a function impact location is not intuitive because tsunami generation depends on ocean bathymetry, which dictates how strongly the Lamb wave couples as it moves along a great circle path. Tsunami run-up distances are a strongly non-linear function of impact location because the coupling and propagation are highly nonlocal and nonlinear. Our results will be compared with other components of the impact damage to assess contribution of this new potential impact.

Keywords: *meteotsunami, Laacher See, Meteor Crater, Tunguska, Krakatau*

Introduction

Much of our understanding of the risk from near-Earth objects comes from the geological record in the form of impact craters, but not all asteroid impacts are crater-forming events. Small asteroids explode before reaching the surface, generating an airburst, and most impacts into the ocean do not penetrate the water to form a crater in the sea floor. The risk from these non-crater-forming ocean impacts and airbursts is difficult to quantify and represents a significant uncertainty in our assessment of the overall threat. We are currently working to better understand impact scenarios that can generate dangerous tsunamis. We suggest that paleo tsunami deposits might be the only evidence in the geological record of past airbursts and ocean impacts that left no other mark, and that it might be possible to test this hypothesis by linking such deposits to known impact structures or explosive volcanic eruptions.

Air-coupled tsunamis

One of the suggested mechanisms for the production of asteroid–generated tsunamis is by direct coupling of the pressure wave to the water, analogous to the means by which a moving weather front can generate a meteotsunami. The strong-est and most destructive meteotsunamis are generated by atmospheric pressure oscillations with amplitudes of only a few hPa (mbar), corresponding to changes in sea level of a few cm. The resulting wave is strongest when there is a resonance between the ocean and the atmospheric forcing. A Proudman resonance takes place when the atmospheric disturbance's translational speed (U) equals the longwave phase speed of a shallow water wave. Coupling is strongest when the Froude number (Fr=U/c) is unity. A weather front propagates much slower than the speed of sound, so meteotsunamis are most common and dangerous in shallow bodies of water such as the Mediterranean Sea or Lake Michigan.

By contrast, the blast wave from an airburst or crater-forming impact propagates at a speed faster than a tsunami in the deepest ocean, and a Proudman reso-nance cannot be achieved even though the overpres-sures are orders of magnitude greater than for a weather front. However, blast wave profiles are N-waves in which a shock wave leading to overpressure is fol-lowed by a more gradual rarefaction to a much longer-duration underpressure phase. Even though the blast outruns the water wave it is forcing, the tsunami con-tinues to be driven by the out-of-resonance gradient associated with the suction phase, which may depend strongly on the details of the airburst or impact scenario.

Prior to the January 15, 2022 explosive eruption of Hunga Tonga-Hunga Ha'apai, the understanding of within the planetary defense community was that the mechanisms for air-driven tsunamis only acted in the vicinity of the impact or airburst, because the pressure and wind disturbances created by the blast wave or other suggested mechanisms (e.g. plume ejection and collapse, steam blowoff, expanding toroidal vortices) decayed rapidly with distance from ground zero, and none of these disturbances propagated at the resonant velocity except under rare conditions [1]. However, the Tonga eruption was powerful enough to generate a Lamb wave that

extended to the top of the atmosphere, propagated at resonant or near-resonant speed in deep water, had a long period that allowed it to drive tsu-nami waves over a long fetch, and decayed so slowly that it traversed the entire globe multiple times. Tsu-namis were observed in other ocean basins separated by continents (e.g. the Caribbean) and could only have been driven by atmospheric disturbances.

Global Lamb-wave Tsunamis

We have run simulations of tsunamis driven by Lamb waves generated by various explosive sources at various geographic locations, including volcanic eruptions, airbursts, and impacts. We used the CTH hydrocode to model the
scenarios and to scale the resulting Lamb wave to generate time dependent boundary conditions as input to shallow-water wave propagation codes. Sources of include volcanos (Tonga, Krakatau, Laacher See, and Toba) and impacts (the hypothetical 2023 PDC asteroid). Because global Lamb Waves can be generated by sources that are nowhere near the ocean, tsunamis can result from crater-forming impacts and airbursts over land. Simulations of potential tsunamis from Meteor Crater and Tunguska are underway. Figures 1 and 2 show calculated maps of the peak tsunami amplitudes resulting from the Tonga and Krakatau explosions.

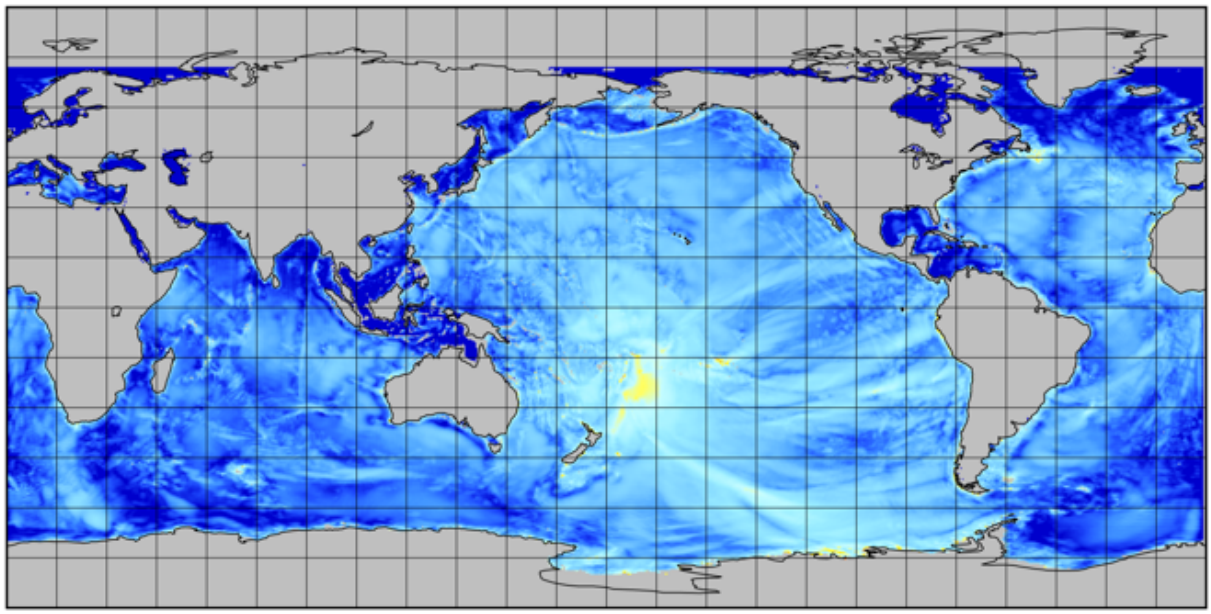

Figure 1 *Map of calculated peak tsunami amplitudes from 2022 Tonga explosion. Similar maps can be generated for Lamb-wave coupled tsunamis generated by known impact or airburst events such as Meteor Crater or Tunguska, for hypothetical impacts such as 2025 PDC, or for potential impacts from real NEOs such as 2024 YR4.*

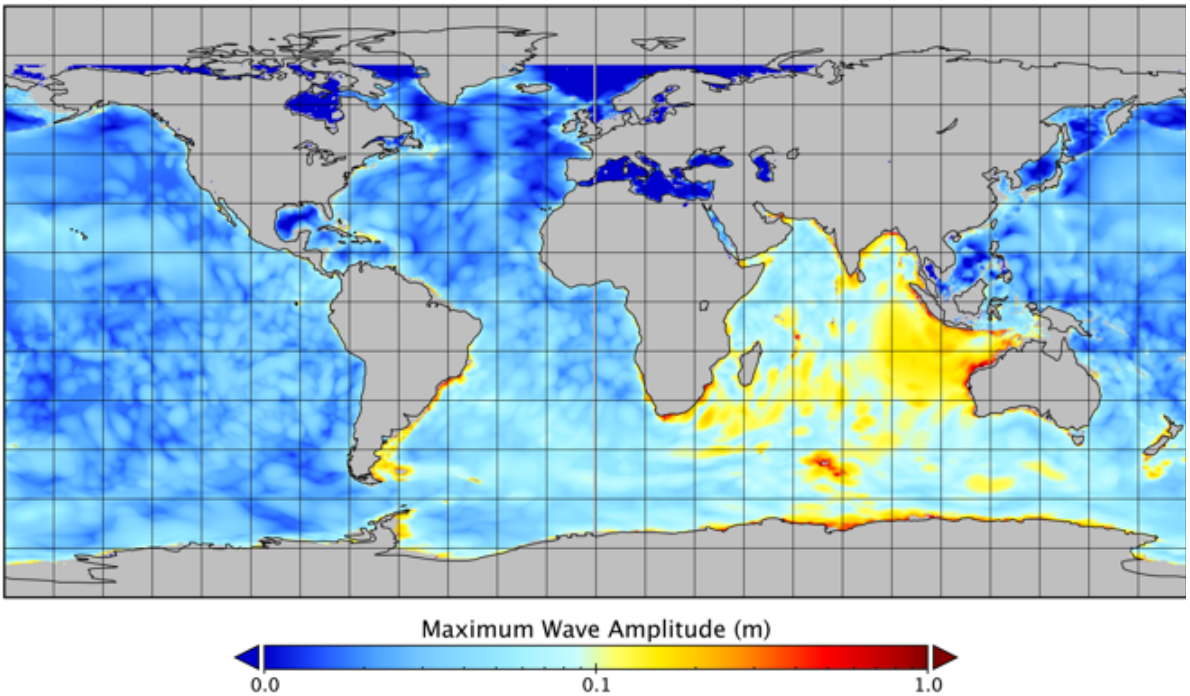

Figure 2 *Map of calculated peak tsunami amplitudes from 1883 Krakatau explosion.*

Explosive coupling efficiency

Our preliminary simulations have shown, as expected, that volatile content of a volcanic magma or impact target rocks govern the efficiency by which the explo-sion transfers energy to the Lamb wave. For a given explosive yield, atmospheric wave amplitudes increase with water content of a magma (Figure 3). We expect that the Lamb wave from Meteor Crater would have high coupling efficiency due to carbonate-rich Kaibab Limestone and water-saturated Coconino Sandstone, and would therefore yield larger tsunamis than an impact of the same magnitude into target rocks that are volatile poor.

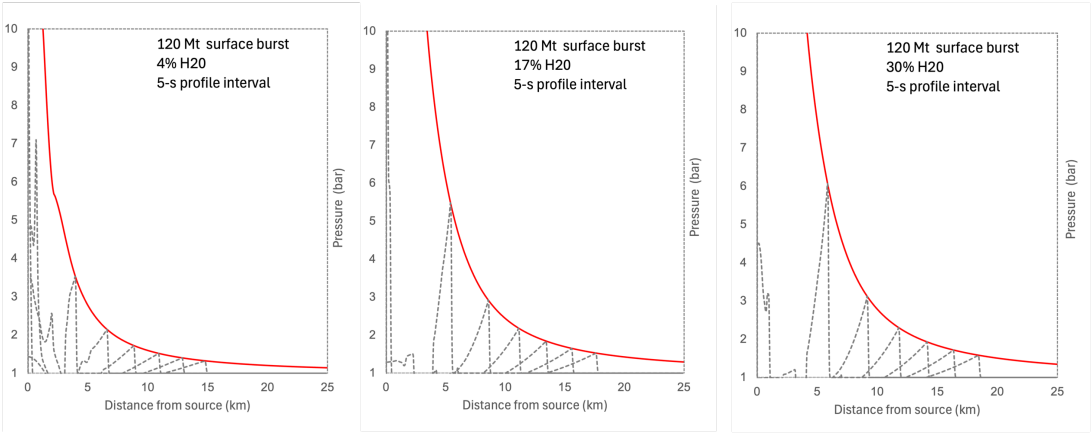

Figure 3. Intensity of explosive volcanic pressure wave depends on source volatile content. CTH simulations of 120 Mt magma explosions show that pressure wave amplitude increases with volatile content. This suggests that volatile-rich of target rocks generate stronger waves from impacts.

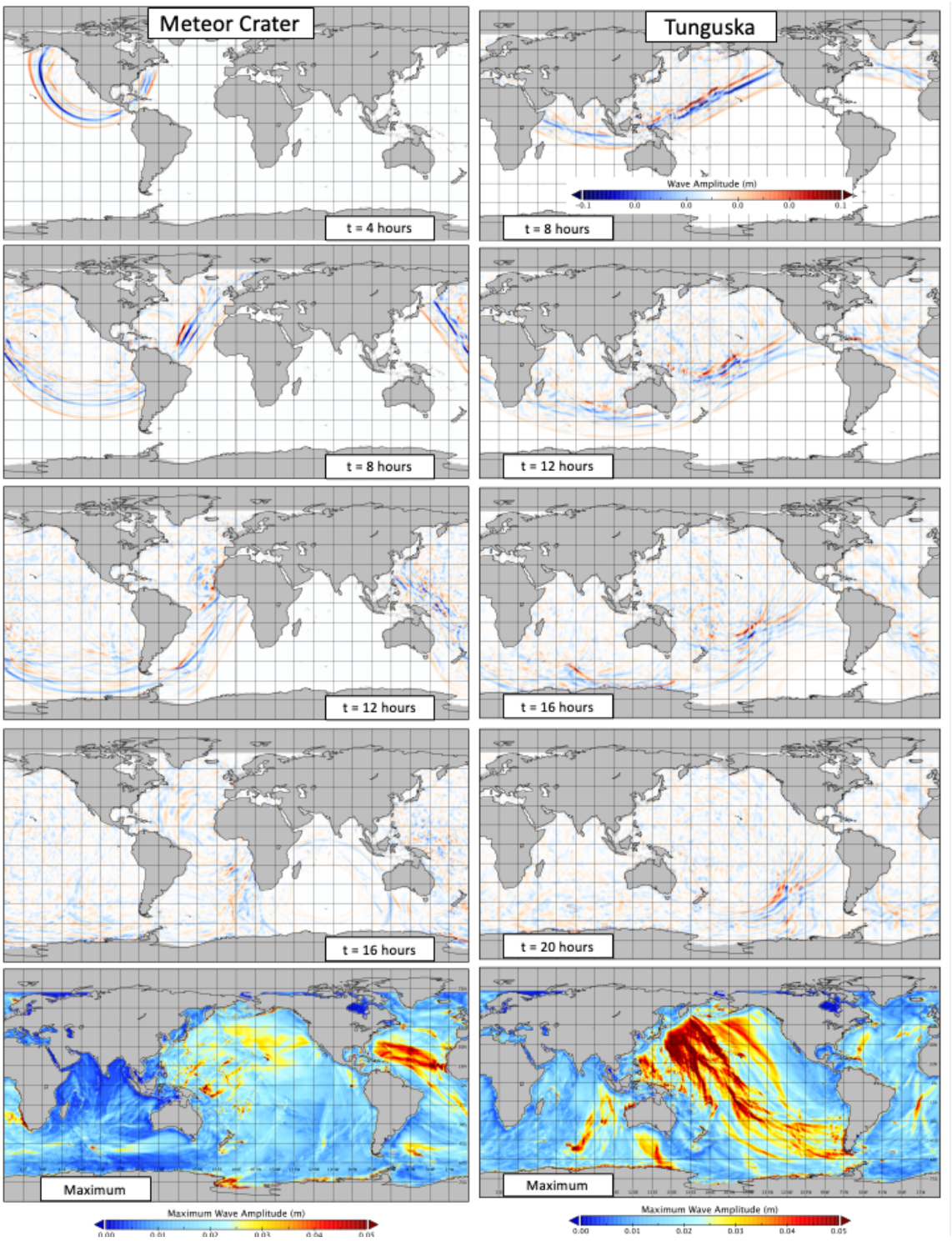

Figure 4. Models of Lamb-wave-driven tsunami generated by a VEI 7+ explosion at location of Meteor Crater (left) and Tunguska (right).

Global tsunami fingerprints

We suggest that this hypothesis can be tested by per-forming tsunami simulations for recent (Quaternary) known large explosive events (both impact and volcan-ic) in the geological record with known timing and source locations, and generating maps of peak tsunami amplitudes around the world. These maps will reveal the likely locations and ages of Lamb-wave coupled tsunami deposits from these events, which would pro-vide confirming evidence for the hypothesis if found at the predicted locations with the right ages.

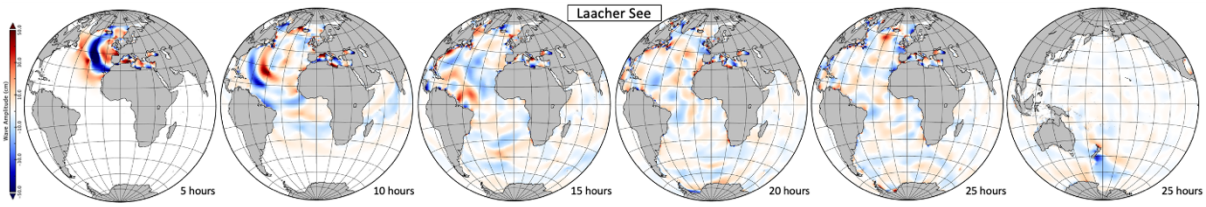

Figure 5. Model of Lamb-wave-driven tsunami generated by a VEI 7+ explosion at location of Laacher See in present-day western Germany. The actual magnitude estimate of the 13 ka BP eruption is VEI 6, so this simulation should be considered an upper bound on the size of the resulting global tsunami. Maximum amplitudes of about 5 meters occur near Iceland, South Americ5, and in the Mediterranean. High amplitudes also occur along Greenland and the eastern margin of the Laurentide ice sheets. The antipode, near New Zealand, also experiences large waves. Paleotsunami deposits in of the correct age in these locations could be evidence for this event.

Conclusions

Lamb-wave driven tsunamis from large explosions (volcanos, impacts, and airbursts) might represent a significant component of overall risk from these natural hazards. Our simulations can inform risk assessments for hypothetical impact scenarios (2025 PDC) as well as real-world objects (2024 YR4). Opportunities for model validation are rare. So far, the only confirmed Lamb-wave generated tsunamis are from the 2022 eruption of Hunga Tonga-Hunga Ha'apai and the 1883 Krakatau eruption. Simulations suggest similar tsunamis were generated by the Tunguska airburst in 1908. Our models also suggest that tsunamis were generated from the Meteor Crater impact as well as the Laacher See volcanic eruption. Larger impacts and volcanic eruptions would be expected to have left paleotsunami deposits that we suggest could be used as a means of model validation for risk assessment associated with planetary defense as well as volcanic hazards.

References

[1] Boslough, M. B. and Titov, V. (2024) Acta Astronautica, 222, 641-646.

MB was supported by the US Department of Energy through the Los Alamos National Laboratory. Los Alamos National Laboratory is operated by Triad National Security, LLC, for the National Nuclear Security Administration of U.S. Department of Energy (Contract No. 89233218CNA000001).